ISSN: 2414-1895 DOI: 10.6919/ICJE.202505_11(5).0030

The Heterostructure of MoS_2 and $CoMoO_4$ for Efficient Oxygen Evolution Reaction at High Current Densities.

Junjie Zheng[a], Chengcheng Yang[b]

School of Materials and Chemistry, University of Shanghai for Science and Technology, Shanghai 200093, China

[a]z63110705@163.com, [b]ycc455150@163.com

Abstract

To investigate the OER performance of MoS_2-based composite electrocatalysts at high current densities, a MoS_2@$CoMoO_4$/CC heterostructured electrocatalyst was successfully constructed via a two-step hydrothermal method. Characterization results demonstrate that the three-dimensional porous architecture composed of ultrasmall nanosheets significantly increases the electrode's effective surface area while facilitating rapid electrolyte penetration, thereby ensuring optimal contact between reactants and electrocatalytic active sites. The formed MoS_2/$CoMoO_4$ heterointerface promotes interfacial charge transfer and accelerates electron migration, effectively reducing the energy barrier for electrochemical reactions. Consequently, the MoS_2@$CoMoO_4$/CC exhibits exceptional OER performance at high current densities.

Keywords

Oxygen Evolution Reaction; Heterostructure; Transition Metal; Electrochemistry.

1. Introduction

Transition metal oxides (TMOs) have been extensively studied as electrocatalysts for the oxygen evolution reaction (OER) due to their cost-effectiveness and abundant reserves. Among them, molybdate-based transition metal materials have attracted particular attention owing to their excellent redox properties, robust structural stability, and high electronic conductivity[1]. Of the various molybdate materials, cobalt molybdate ($CoMoO_4$, CMO) is considered a highly promising electrocatalyst due to its high intrinsic activity, which arises from the synergistic effect between the superior redox properties of cobalt and the enhanced conductivity of molybdenum[2, 3]. Molybdates can be easily grown in rod-like, sheet-like, or other morphologies on substrates such as nickel foam or carbon cloth, forming self-supporting electrodes that exhibit outstanding performance at high current densities[4]. However, compared to noble metal-based electrocatalysts, the electrocatalytic performance of CMO still falls short. Research by Prof. Yang Xiurong[5] successfully prepared three-dimensional nanoflower-structured $CoMoO_4$ and its Fe-doped modified material (CFMO) electrocatalyst via a one-step hydrothermal method. The study innovatively revealed that the introduction of Fe disrupts the original balance of Co-O-Co bonds, forming a shorter-bonded Co-O-Fe oxygen-bridge structure. This unique Co-O-Fe bimetallic site possesses an optimized electronic structure, effectively promoting the direct coupling of oxygen radicals and significantly enhancing catalytic performance. As a result, the CFMO catalyst demonstrated exceptional OER activity in alkaline media, requiring only 217 mV overpotential to achieve a current density of 10 mA cm^{-2} and 257 mV for 50 mA cm^{-2}. Moreover, the catalyst exhibited excellent stability over 1000 hours of continuous operation. When assembled into an anion exchange membrane (AEM) electrolyzer, it achieved a high current density of 1.0 A cm^{-2} at just 1.65 V. Prof. Qian Dong[6] developed an Fe-P

ISSN: 2414-1895 DOI: 10.6919/ICJE.202505_11(5).0030

co-doped $CoMoO_4$ (Fe-P-CMO) electrocatalyst for efficient overall water splitting. The study found that during the OER process, the catalyst undergoes significant structural evolution, with complete dissolution of Mo leading to deep reconstruction of the P-doped $CoMoO_4$, ultimately transforming in situ into a highly active Fe_2O_3/CoOOH heterostructure. In contrast, during the hydrogen evolution reaction (HER), the active sites were identified as Fe_2O_3/$Co(OH)_2$/P-$CoMoO_4$. This heterointerface structure not only significantly improves electron transfer efficiency but also greatly enhances intrinsic electrochemical activity through multi-component synergy. The Fe-P-CMO(−)||Fe-P-CMO(+) overall water-splitting system (1 M KOH) required ultralow cell voltages of only 1.48 V and 1.59 V to achieve current densities of 10 mA cm^{-2} and 100 mA cm^{-2}, respectively, demonstrating outstanding electrocatalytic performance.

Building upon these insights, to explore the application of MoS_2-based composite materials in OER at high current densities, this study employed a two-step hydrothermal method. First, $CoMoO_4$ nanosheet arrays were synthesized on a carbon cloth substrate, followed by a secondary hydrothermal process to form a heterostructure of MoS_2 and $CoMoO_4$. The construction of this heterostructure effectively modifies the electronic structure of the catalyst, accelerates charge transfer, and thereby promotes the OER process. Additionally, the three-dimensional porous structure composed of ultra-thin nanosheets facilitates rapid electrolyte penetration at high current densities, ensuring sufficient contact between reactants and electrocatalytic active sites while enabling fast bubble release. After optimization, the prepared MoS_2@$CoMoO_4$/CC required only 294 mV overpotential to achieve 100 mA cm^{-2} with outstanding stability, and merely 364.1 mV for 500 mA cm^{-2}. When assembled into an AEM electrolyzer, it required only 1.78 V to reach 100 mA cm^{-2} at room temperature, and just 1.93 V for a high current density of 500 mA cm^{-2}.

2. Material and Methods

2.1 Sample Preparation

The synthesis of MoS_2@$CoMoO_4$/CC was achieved through the following hydrothermal reaction. First, 0.3 mmol of $(NH_4)_6Mo_7O_{24}\cdot 4H_2O$ and 10 mmol of thiourea were dissolved in 25 mL of deionized water and stirred for 30 minutes to form a homogeneous clear solution. The solution was then transferred into a Teflon-lined autoclave, and a pre-prepared $CoMoO_4$/CC electrode (2 × 3 cm^2) was vertically immersed into it. The reaction proceeded at 180°C for 24 hours. After completion, the as-prepared MoS_2@$CoMoO_4$/CC was taken out and repeatedly washed with deionized water and ethanol several times. Finally, the MoS_2@$CoMoO_4$/CC electrode was vacuum-dried at 60°C for 12 hours.To investigate the effect of the MoS_2-to-$CoMoO_4$ feeding ratio on the OER catalytic activity, electrocatalysts with MoS_2:$CoMoO_4$ molar ratios of 1:2, 2:1, and 3:1 were also prepared under identical conditions for comparison.

2.2 Characterization

X-ray diffraction (XRD) patterns were performed on Bruker D8 Advance with Cu Kα radiation (λ = 0.15418 nm) in the range of 5° to 65° at a scanning speed of 5° min^{-1}. Raman spectroscopy was obtained on a Thermo Fischer DXR Raman spectrometer with 532 nm solid laser as an excitation source. The scanning electron microscopy (SEM) images were obtained from a JSM-7800F electron microscope, and the microscope was operated at 20 kV. The electrochemical performance tests were performed on a CHI660E electrochemical workstation. All tests adopted a three-electrode system. OER tests was carried out in the N2-saturated 1.0 M KOH solution, the prepared MoS_2@$CoMoO_4$/CC (active area of 1cm×1cm×2) was used as working electrodes, graphite rods as counter electrodes and Hg/HgO as reference electrodes. Linear scanning voltammetry (LSV) was performed at 5 mV s−1 to evaluate the performance of OER from 0 to 1 V. Before LSV testing, the catalyst samples were electrochemically activated in 1.0 M KOH using CV cycling at 50 mV/s for 40 consecutive cycles in a conventional three-electrode cell. Electrochemical impedance spectroscopy (EIS) was measured from 0.01 Hz to 100 kHz. The Tafel slope was calculated based on the Tafel equation.

ISSN: 2414-1895 DOI: 10.6919/ICJE.202505_11(5).0030

3. Results and discussion

3.1 Preparation of MoS_2@$CoMoO_4$/CC electrocatalyst

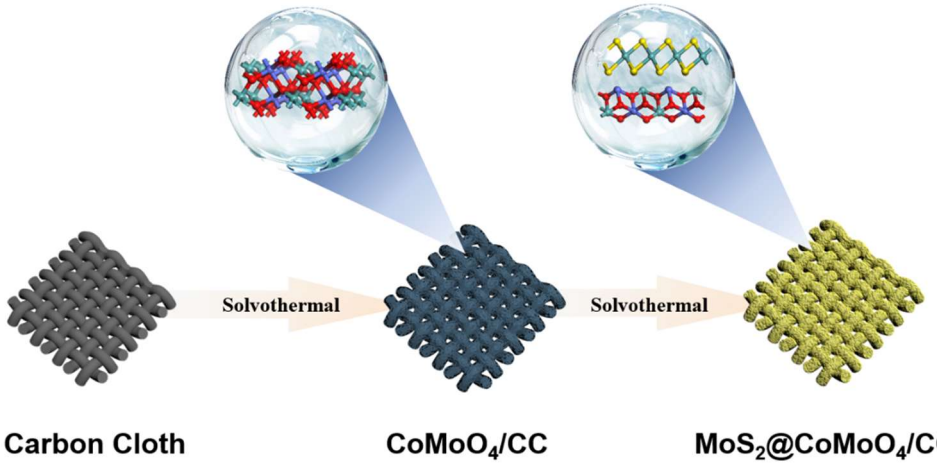

Figure 1. Schematic illustration of the synthesis process for MoS_2@$CoMoO_4$/CC.

Figure 1 illustrates the fabrication process of MoS_2@$CoMoO_4$. Initially, $CoMoO_4$ nanosheet arrays were hydrothermally synthesized on a carbon cloth substrate. Subsequently, a secondary hydrothermal process was employed to obtain a structure where MoS_2 nanospheres uniformly cover the $CoMoO_4$ nanosheets. The well-ordered nanosphere architecture significantly enhances the oxygen evolution reaction (OER) performance.

3.2 Morphological Analysis of MoS_2@$CoMoO_4$/CC

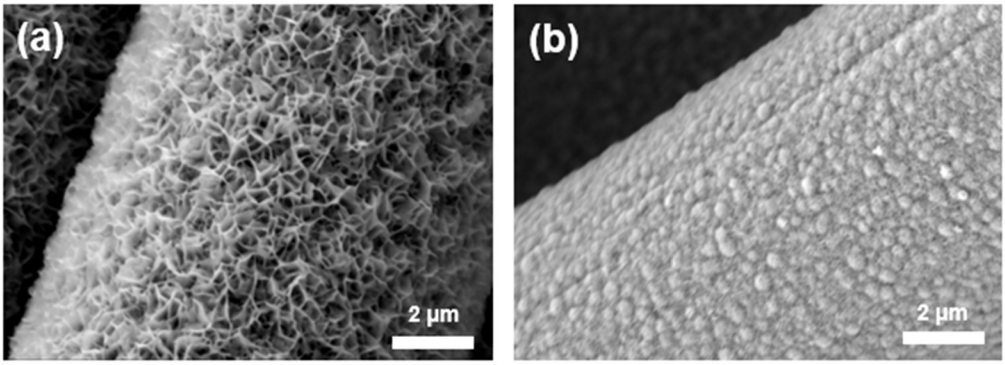

Figure 2. SEM images of (a) $CoMoO_4$/CC and (b) MoS_2@$CoMoO_4$/CC.

The morphology and structure of MoS_2@$CoMoO_4$/CC were first characterized by scanning electron microscopy (SEM). As shown in Figure 2 (a), the $CoMoO_4$ nanosheet arrays grow uniformly on the carbon cloth surface. These ultrathin nanosheets exhibit extremely small dimensions (less than 1 μm) and self-assemble into a three-dimensional porous architecture. This unique structure not only significantly increases the specific surface area of the catalyst but also facilitates rapid electrolyte penetration, ensuring sufficient contact between reactants and electrocatalytic active sites.After MoS_2 incorporation, Figure 2(b) reveals that the catalyst-loaded carbon fibers maintain a relatively smooth overall morphology. However, high-resolution SEM images (Figure 5-2d) clearly demonstrate that the $CoMoO_4$ nanosheets are decorated with nanosphere structures composed of even finer nanosheets. Due to their extremely small size, these nanospheres are not distinctly observable in low-magnification SEM images. Compared to $CoMoO_4$/CC, this hierarchical nanostructure with finer nanospheres exposes more active surface area and reaction sites, thereby endowing the MoS_2@$CoMoO_4$/CC composite with superior electrochemical performance.

ISSN: 2414-1895 DOI: 10.6919/ICJE.202505_11(5).0030

3.3 Structural Analysis of MoS_2@$CoMoO_4$/CC

To determine the crystal structure of the synthesized electrocatalytic materials, the samples were characterized by XRD. As shown in Figure 3(a), $CoMoO_4$ exhibits weak crystallinity with diffraction peaks appearing at 2θ = 33.5°, 36.14°, 39.3°, and 58.5°, corresponding to the ($\bar{2}22$), (400), (040), and (024) planes of $CoMoO_4$ (JCPDS No. 21-0868), respectively. The broad peak around 25.5° represents the carbon peak from the carbon cloth substrate. After the introduction of MoS_2, diffraction peaks at 2θ = 13.5°, 32.2°, and 57.5° can be observed, corresponding to the (002), (100), and (110) crystal planes of MoS_2, respectively. Notably, compared to the MoS_2 PDF card (JCPDS No. 37-1492), the (002) diffraction peak of the MoS_2@$CoMoO_4$/CC catalyst shows a slight shift of less than 1°, which may be attributed to lattice strain and increased interlayer spacing caused by interfacial stress between the MoS_2 layers and $CoMoO_4$[7].The phase composition of the prepared samples was further characterized by Raman spectroscopy (Figure 3b). For the $CoMoO_4$/CC sample, a broad peak at 334.4 cm-1 is observed, corresponding to the characteristic vibrational peak of the Co-Mo-O bond in $CoMoO_4$[8]. For pure-phase MoS_2/CC, the peaks at 377.3 cm^{-1} and 407.4 cm^{-1} correspond to the in-plane and out-of-plane vibrational modes of 2H-phase MoS_2, respectively. Compared to MoS_2/CC, MoS_2@$CoMoO_4$/CC exhibits additional characteristic peaks at 231.9 cm^{-1}, 282.4 cm^{-1}, and 336.2 cm^{-1}, which are associated with the characteristic phonon vibrational modes of 1T-phase MoS_2. Moreover, the intensity of the characteristic peaks of the 2H-phase at 375.5 cm^{-1} and 403.9 cm^{-1} is significantly reduced. This indicates that during the preparation of the composite material, a portion of the 2H-phase MoS_2 underwent a phase transition, forming a 1T-phase structure with higher conductivity.

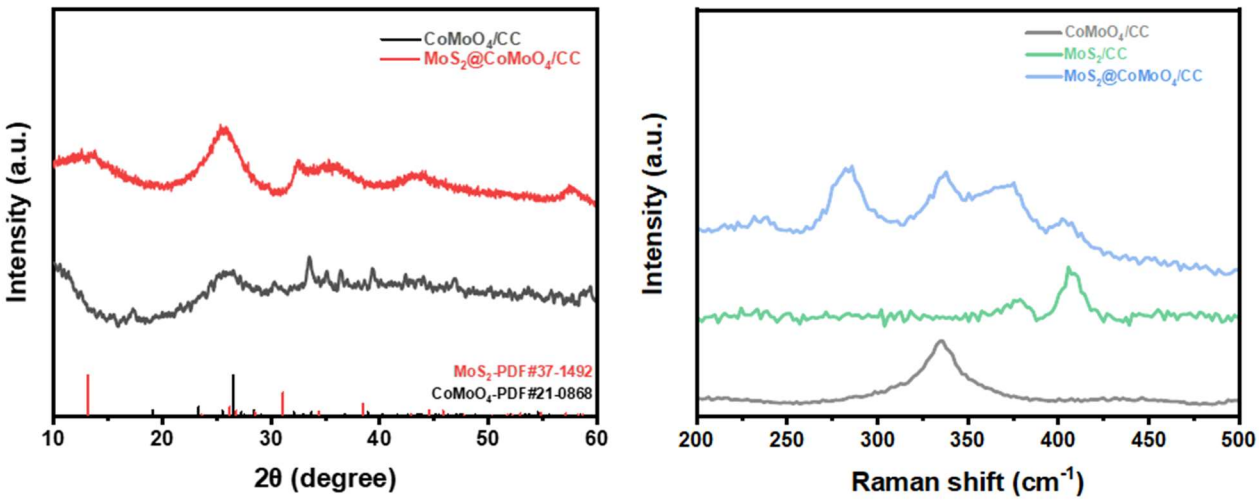

Figure 3. (a) XRD patterns of $CoMoO_4$/CC and MoS_2@$CoMoO_4$/CC, (b) Raman spectra of $CoMoO_4$/CC, MoS_2/CC, and MoS_2@$CoMoO_4$/CC.

3.4 Performance Analysis of MoS_2@$CoMoO_4$/CC

The linear sweep voltammetry (LSV) curves of all electrocatalysts were measured in a three-electrode system using 1.0 M KOH electrolyte at a scan rate of 5 mV s^{-1}. As shown in Figure 4(a), since MoS_2@$CoMoO_4$/CC exhibits distinct oxidation peaks in the LSV curves, the overpotentials were compared at a current density of 100 mA cm^{-2}. The heterostructure of MoS_2@$CoMoO_4$/CC catalysts was further investigated by adjusting the Mo:Co ratios. Remarkably, the MoS_2@$CoMoO_4$/CC catalyst with a Mo:Co ratio of 2:1 demonstrates optimal OER performance, requiring only 294.2 mV overpotential to achieve 100 mA cm^{-2} current density. This performance significantly surpasses other ratio samples: Mo:Co = 1:1 (302.5 mV), 3:1 (316.1 mV), 1:2 (379.5 mV), and pure $CoMoO_4$/CC (390.0 mV). The optimized MoS_2@$CoMoO_4$/CC electrocatalyst maintains excellent activity even at high current density (500 mA cm^{-2}), requiring merely 364.1 mV. Notably, the electrocatalytic performance initially enhances then weakens with increasing Mo content, while pure-phase MoS_2/CC shows negligible OER activity.The exceptional catalytic performance originates from synergistic

ISSN: 2414-1895 DOI: 10.6919/ICJE.202505_11(5).0030

effects at the MoS_2@$CoMoO_4$/CC heterointerface, where electronic interactions optimize the material's electronic structure and facilitate interfacial charge transfer, thereby significantly enhancing catalytic activity. The optimized Mo/Co ratio creates the most favorable electronic structure for lowering the OER energy barrier.To gain deeper insight into the OER kinetics, Tafel slopes were derived from LSV curves (Figure 4 b-c). The 2:1 Mo:Co ratio catalyst exhibits the smallest Tafel slope (78.9 mV dec-1), outperforming other ratios (1:1: 81.7 mV dec_{-1}; 3:1: 85.8 mV dec^{-1}; 1:2: 133.8 mV dec-1) and pure $CoMoO_4$/CC (152.6 mV dec^{-1}). The lower Tafel slope indicates faster reaction kinetics for the 2:1 ratio catalyst, further confirming its superior OER activity.Electrochemical impedance spectroscopy (EIS) measurements with equivalent circuit fitting (Figure 4d) reveal that the 2:1 Mo:Co ratio catalyst displays the smallest semicircle radius in Nyquist plots, corresponding to the lowest charge transfer resistance (R_{ct}). This demonstrates enhanced charge transfer capability, where abundant heterointerfaces effectively reduce interfacial charge transport resistance and accelerate electron transfer during OER processes.

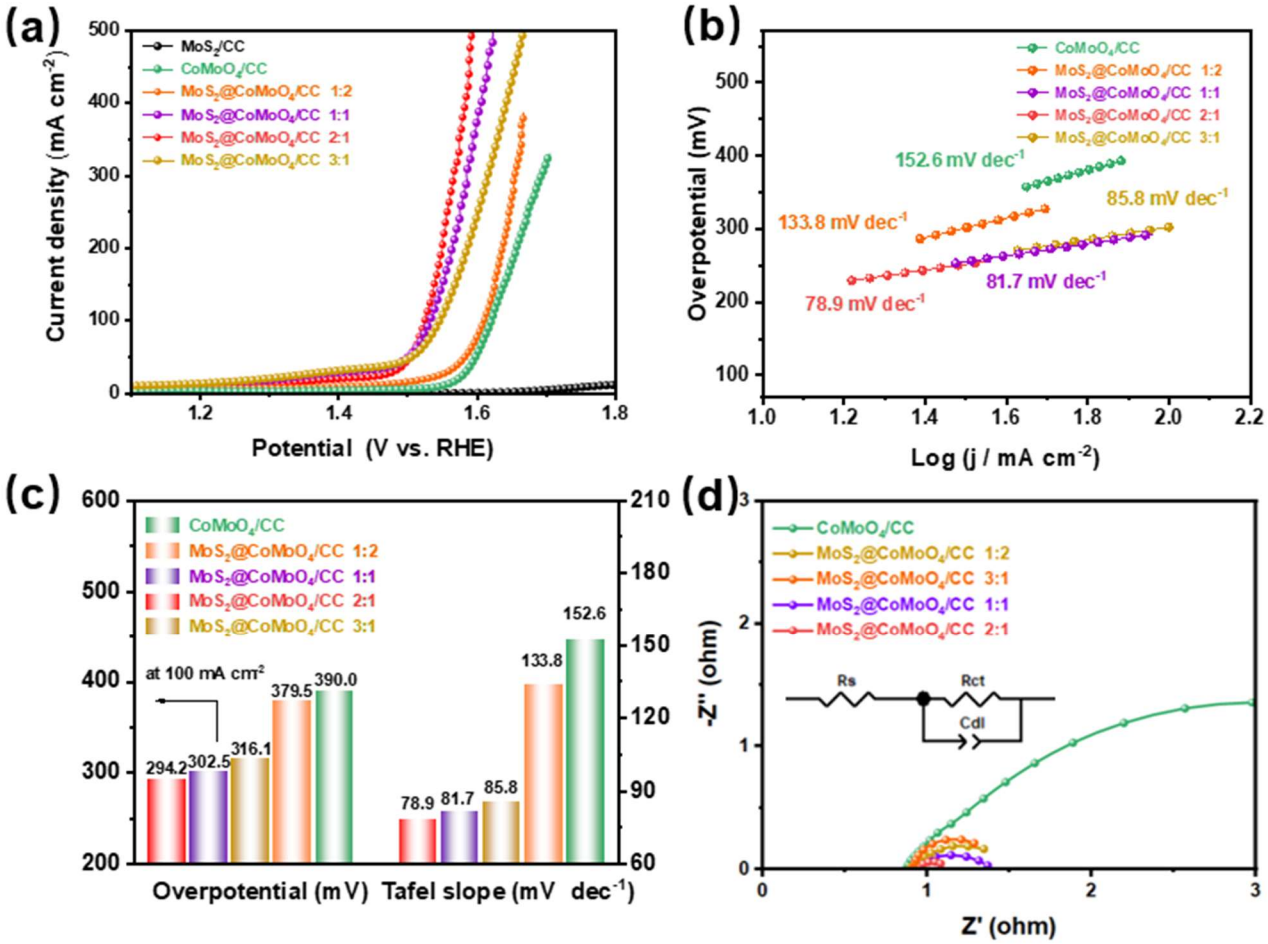

Figure 4. (a) LSV curves of MoS_2/CC, $CoMoO_4$/CC, and MoS_2@$CoMoO_4$/CC with different synthesis ratios in 1.0 M KOH; (b) Tafel slopes of different catalysts; (c) Comparison of overpotentials at 10 mA cm^{-2} and Tafel slopes for the catalysts; (d) Nyquist plots.

4. Conclusion

Based on the aforementioned research findings, this study successfully constructed a MoS_2@$CoMoO_4$/CC heterostructure electrocatalyst through a two-step hydrothermal synthesis method: First, $CoMoO_4$ nanosheet arrays were grown in situ on carbon cloth substrate, followed by a secondary hydrothermal reaction to grow MoS_2 nanospheres on their surface. Electrochemical tests demonstrate that this catalyst exhibits outstanding oxygen evolution reaction (OER) performance,

ISSN: 2414-1895 DOI: 10.6919/ICJE.202505_11(5).0030

with its exceptional catalytic activity primarily attributed to the following factors: The three-dimensional porous structure composed of ultra-small nanosheets in the prepared MoS_2@$CoMoO_4$/CC electrocatalyst effectively increases the electrode's surface area, promotes rapid electrolyte penetration, and facilitates sufficient contact between reactants and electrocatalytic active sites. The metallic 1T-phase MoS_2 possesses superior conductivity compared to the 2H-phase MoS_2, thereby favoring electron transfer during the oxygen evolution reaction. The heterostructure formed between MoS_2 and $CoMoO_4$ promotes interfacial charge transfer, accelerates interfacial electron migration, and consequently reduces the energy barrier for electrochemical reactions. The prepared MoS_2@$CoMoO_4$/CC electrocatalyst demonstrates remarkable OER performance, requiring only 294.2 mV overpotential at 100 mA cm^{-2} current density while exhibiting excellent durability. Even at a high current density of 500 mA cm^{-2}, it requires merely 364.1 mV. When assembled into an AEM electrolyzer, it achieves 100 mA cm^{-2} at only 1.78 V under room temperature conditions, and maintains just 1.93 V cell voltage at the high current density of 500 mA cm^{-2}.

References

[1] Barik S, Kharabe G P, Illathvalappil R, et al. Active Site Engineering and Theoretical Aspects of "Superhydrophilic" Nanostructure Array Enabling Efficient Overall Water Electrolysis [J]. Small, 2023, 19(50): 2304143.

[2] Jiang T, Xie W, Geng S, et al. Constructing oxygen vacancy-regulated cobalt molybdate nanoflakes for efficient oxygen evolution reaction catalysis [J]. Chinese Journal of Catalysis, 2022, 43(9): 2434-2442.

[3] Wang K, Li Y, Hu J, et al. Deep reconstruction of transition metal molybdate@hydroxide heterostructure triggered by anion-exchange reaction as high efficiency water oxidation electrocatalyst [J]. Chemical Engineering Journal, 2022, 447: 137540.

[4] Chang Y, Lu X, Wang S, et al. Built-In Electric Field Boosted Overall Water Electrolysis at Large Current Density for the Heterogeneous Ir/CoMoO4 Nanosheet Arrays [J]. Small, 2024, 20(29): 2311763.

[5] Yao B, Chen Y, Yan Y, et al. Iron-Induced Localized Oxide Path Mechanism Enables Efficient and Stable Water Oxidation [J]. Angewandte Chemie-International Edition, 2025, 64(4): e202416141.

[6] Wang B W, Chen X X, He Y J, et al. Fe2O3/P-doped CoMoO4 electrocatalyst delivers efficient overall water splitting in alkaline media [J]. Applied Catalysis B-Environment and Energy, 2024, 346: 123741.

[7] Ye S, Zhang Y, An C, et al. Interfacial-Aligned and High Conductive 1T-MoS2@Ti3C2Tx Heterostructure Nonwoven Fabric for Robust Deformable Supercapacitors [J]. Advanced Functional Materials, 2024: 2419779.

[8] Arumugam B, Siddharthan E E, Mannu P, et al. Regulating the electronic structure of CoMoO4 via La doping for efficient and durable electrochemical water splitting reactions [J]. Journal of Materials Chemistry A, 2025, 13(9): 6749-6767.